Comparison of Three Boundary Detection Methods for SPECT Using Compton Scattered Photons

D.J. Macey, G.L. DeNardo, and S.J. DeNardo

Departments of Radiology and Internal Medicine, University of California, Davis Medical Center, Sacramento, California

Three simple methods of defining the boundary of a transverse section in single photon emission computed tomography (SPECT) were compared using Compton scattered photons from a small ^{99m}Tc source located either inside or outside a water-filled cylinder of 22 cm diameter. Scattered events were acquired with 360-degree rotation of the gamma camera and transverse section images were reconstructed using a filtered backprojection method. The boundary of section images obtained with three different geometric arrangements of the source and the camera were compared. The 90-degree Compton scatter method, using a source external to the cylinder and at 90° to the front of the detector, was found to give the best boundary definition. Similarly, detection of scattered events using a radionuclide source placed outside a human body was capable of providing good boundary information for the large stack of contiguous section images produced by a rotating SPECT camera. Calculations confirmed the profound influence of boundary errors on SPECT quantitations.

J Nucl Med 29:203–207, 1988

Rigorous attenuation compensation methods for quantitative single photon emission computed tomography (SPECT) require accurate information for the boundary, the attenuation coefficients and the edges of organs of differing density in each transverse section image (*1,2*). For section images of the head or abdomen, only the section boundary is required because of the predominantly uniform tissue density of these areas of the body and usually an elliptical contour is assumed for most attenuation compensation methods that are currently used (*3*).

A Compton scatter method has been described that provides section boundary information from the reconstruction of scattered events emanating from the source in the section (*4*). An isocount thresholding method can sometimes be used on the reconstructed transverse section image if a reasonable fraction of the administered radionuclide is distributed in blood pool or some other widely distributed space in the body (*5*). More recently, a threshold search routine has been used to find the body contour in reconstructed section images by defining edges with a count threshold. This method was applied to projection images acquired from photopeak events (*6*).

The objective of the present study was to compare boundary information obtained from the reconstruction of Compton scattered events acquired with three different geometric arrangements of the source and gamma camera. Section images reconstructed from projection images obtained from Compton scattered events from a source in the section were compared with those obtained from acquisition of 90-degree and backscattered Compton events. In all cases boundary information was obtained for each section image using standard commercially available reconstruction software.

MATERIALS AND METHODS

A single, large field-of-view, gamma camera designed for SPECT with a low-energy, all purpose collimator and interfaced to a nuclear medicine computer system was used for these studies. The photopeak gamma camera images were acquired using a 20% window for the 140 keV photons emitted by technetium-99m (^{99m}Tc). The Compton scatter window used for gamma camera imaging of each source-detector geometry was chosen to optimize the section boundary information.

Received Jan. 20, 1987; revision accepted July 7, 1987.

For reprints contact: G.L. DeNardo, MD, University of California Davis Medical Center, 4301 X St., FOLB II-E, Sacramento, CA 95817.

For studies of Compton scatter from a source in the section, a 15-ml vial of 2 cm diameter was filled with 10 ml of water containing ~1 mCi of ^{99m}Tc and was fixed at 5.5 cm off axis inside a 22 cm diameter cylindrical water-filled SPECT phantom. For all the scatter experiments, the phantom was placed on the SPECT couch so that ~10 cm extended beyond the end of the couch. The boundary of the SPECT couch was thus omitted from the section images of the phantom. An energy window was centered at 110 keV with a window width of 30% in order to collect scattered events from 94 to 127 keV for this internal scatter geometry (Fig. 1A).

For studies of Compton scattered events from a source outside a transverse section, a 35-ml solution of 10 mCi of ^{99m}Tc in a plastic tube (2 cm in diameter, 12 cm in length) was placed in a closely fitting cylindrical lead container. The container was 13 cm in length and 2 cm in internal diameter with a wall 5 mm thick. A slit 5 mm wide and 10 cm in length was cut along one side of the container to provide a crudely collimated beam of 140-keV photons for subsequent studies either of 90-degree or backscatter geometry. This collimated source was fixed to an adjustable clamp that was bolted to one side of the camera yoke so that it described a 360-degree rotation of the camera around the SPECT couch with a radius of 30 cm. For recording 90-degree Compton scatter projection images, the photons from the slit of the lead container were incident on the 22 cm diameter cylinder in a direction parallel to the face of the collimator of the camera (Fig. 1B). The gamma ray spectrum recorded for this geometry is also shown in Figure 1B. In this case a 20% window centered at 110 keV was used for acquisition of the projection images so that scattered photons from 99 to 121 keV were accepted.

The same clamp was adjusted for studies of backscatter geometry so that the emergent beam of photons from the source of ^{99m}Tc was incident on the object as shown in Figure 1C. The energy window used for this geometry was 10% centered around 90 keV, so that scattered photons from 77 to 104 keV were accepted.

Throughout this study, 64 projection images each of 10–30 sec for 360-degree rotation of the camera were acquired in order to record a minimum of 1,000,000 counts for a complete rotation. A 64 × 64 matrix was used for acquisition so that the pixel and voxel dimensions were 6 mm. All transverse section images were reconstructed using a standard filtered back-projection algorithm after correction for the predetermined error in the axis of rotation. A Butterworth filter with a cutoff of 0.85 times the Nyquist frequency and an order of 16 was used to reconstruct the section images. The sizes of imaged objects were measured using a straight line count profile drawn on the section images. The position of the boundary in the count profile was taken as the pixel with 50% of the local maximum count.

Projection images of the head and abdomen of a human subject were acquired in the same manner as for the cylindrical phantom in order to assess the clinical applicability of the 90-degree Compton scatter boundary detection method.

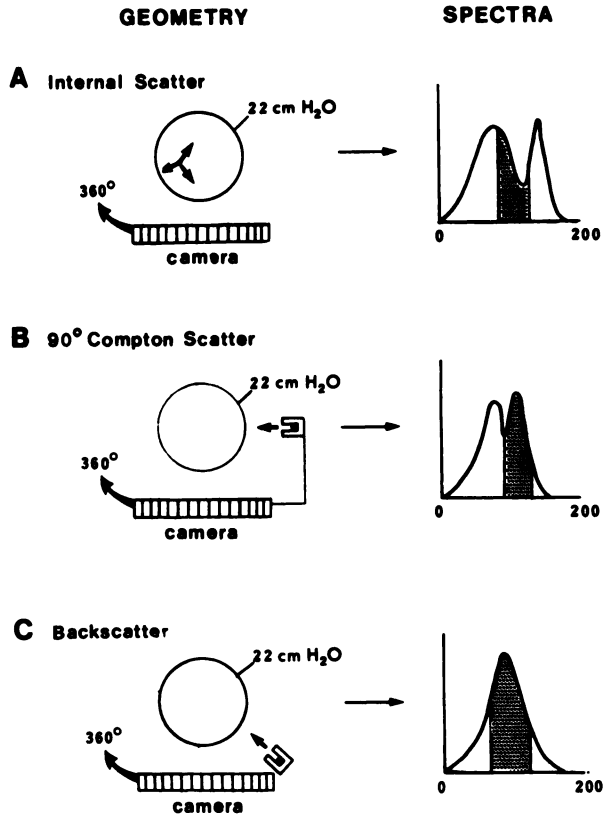

FIGURE 1
Schematic illustration of the three geometric arrangements of the gamma camera and ^{99m}Tc source and the recorded gamma ray spectrum. A: Scatter from the source inside the section; B: 90-degree Compton scatter from source outside the section; and C: Backscatter from the source outside the section.

RESULTS

A typical projection image and straight line count profile across the cylindrical phantom obtained with the three scatter geometries are shown in Figure 2. The slope of the count profile at the boundary of the phantom adjacent to the internal source was less steep for the internal scatter method than that for either external scatter method. At the more distant region of the boundary the internal scatter method provided few events and a shallow slope whereas the entire boundary was clearly defined by both external scatter methods because of the steep slope of the count profile which did not change with rotation of the camera. Corresponding transverse section images obtained from reconstruction of the projection images of the phantom are shown in Figure 3. The diameter of each transverse section was measured from a straight line count profile drawn on the transverse section images. The external scatter methods provided good definition of the whole boundary of the phantom and the measured diameter of the phantom was defined to within one pixel or 6 mm for the 64 × 64 matrix used in these studies.

Sixteen 12 mm thick contiguous transverse section images of the abdomen of a relatively lean male subject obtained with acquisition of 90-degree Compton scatter projection images over 360° are shown in Figure 4.

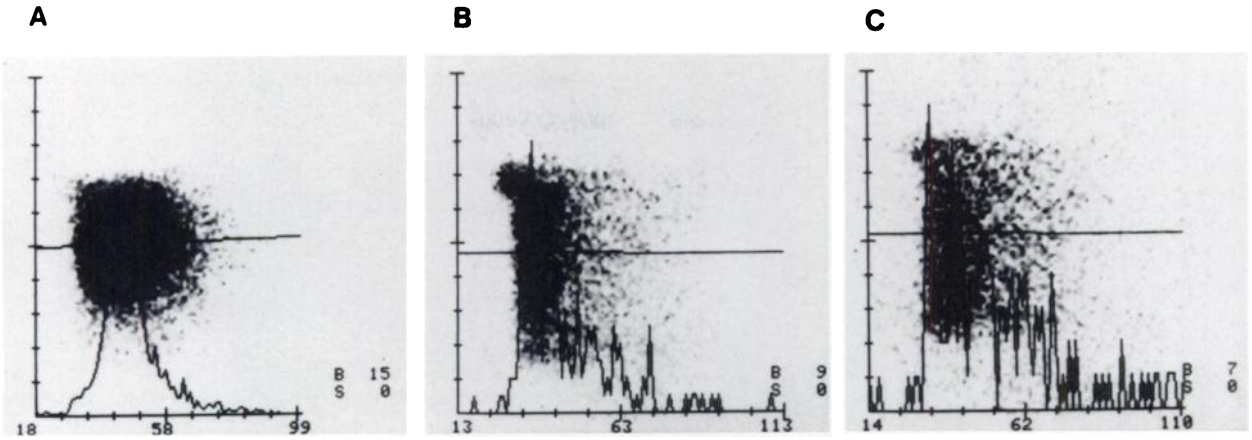

FIGURE 2
Straight line count profiles across a projection image of the cylindrical phantom obtained with A: Internal scatter; B: 90-degree Compton scatter; and C: Backscatter. The slope of the count profile at each boundary of the phantom is reduced for the internal scatter method (A) whereas for the external scatter methods, the slope is steep and defines the boundary equally well in all projection images.

Similarly, 16 section images of the head of the same subject also obtained with 90-degree Compton scatter information are shown in Figure 5. Because of the circular orbit of the camera, the lateral boundaries of the abdomen were closest to the external source and were more clearly defined than were the front and back of the subject.

DISCUSSION

Visual inspection of the section images of the circular phantom provided by the three scatter methods indicated that the 90-degree Compton scatter method provided the best individual section boundaries for a large stack of transverse section images. The diameter of the cylinder measured from the section images provided by the external scatter methods were found to agree with the known phantom dimension to within 6 mm. We recognize that the phantom simulation that was studied represents a special circumstance wherein a radionuclide is not widely distributed in the cross section. This circumstance prevails when radiopharmaceuticals are used that target specific tissues. A classic example is the use of radioiodide to target the thyroid gland or thyroid cancer. Specific targeting is also the goal when radiopharmaceuticals, such as MIBG or monoclonal antibodies are used, albeit these remain to be improved. When a substantial amount of the radiopharmaceutical remains in the vascular or interstitial space, then the boundary of the cross-section can be determined by Compton scatter of internal events or even photopeak events in some instances. However, our experience has been that boundary detection by these approaches is difficult and not accurate enough for quantitative SPECT. With a distributed source there will be an increase in the number of scattered events detected from the boundary generally but the slope of the count

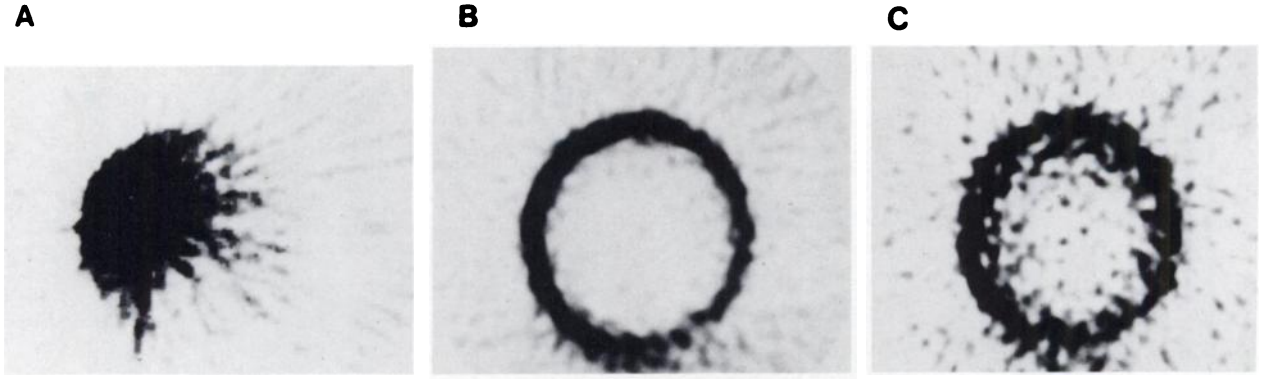

FIGURE 3
Transverse section images of a 22-cm-diameter cylindrical phantom made of lucite and filled with water obtained with reconstruction of the scattered events from: A: Internal scatter; B: 90-degree Compton scatter; and C: Backscatter. The outline of the transverse section obtained from 90-degree Compton scatter is best defined.

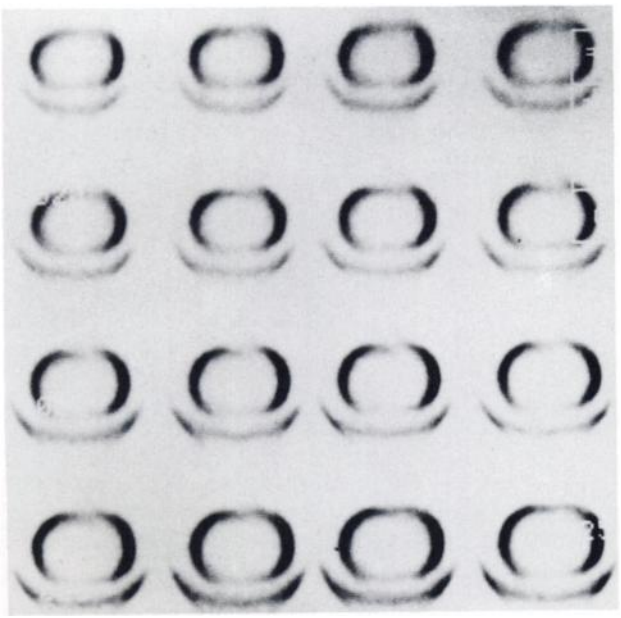

FIGURE 4
Sixteen 12 mm thick contiguous transverse section images of the abdomen of a male subject obtained from reconstruction of the 90-degree Compton scattered events acquired with 360-degree rotation of a ^{99m}Tc source and the gamma camera. The boundaries of the abdomen (and the couch) are well defined.

profile cannot match that provided by the external scatter methods.

Both external Compton scatter methods are easy to apply in clinical practice since no special image processing is required and the usual reconstruction methods can be used. Scatter from radionuclide within a patient will represent only a small fraction of detected scatter events from the external source, thereby not interfering with the method. Construction of the clamp and slit collimator assembly was comparatively easy and did not influence the counterbalance of the SPECT camera gantry. Camera-computer systems capable of simultaneous acquisition of two windows of different photon energy will make the method easy and efficient to apply in a routine clinical environment. The additional radiation absorbed dose from this procedure is small. With a 10 mCi source of ^{99m}Tc at a mean distance of 10 cm from the skin surface of a subject, the radiation absorbed dose to the skin is estimated to be <20 mrad for the 10 to 20 min required to acquire projection images over 360° of rotation.

Body contour errors, such as those introduced by the assumption of an approximate ellipse, have been found to be a source of noise for SPECT (*7*). Investigation by computer simulation led others to the conclusion that the impact of errors in boundary information was more significant for image quantitation than for image appearance (*7*). The present study has shown that boundary information for individual sections can be provided by the 90-degree Compton scatter method for a stack of slices of the body so that the count information in each section can be independently and accurately corrected for photon attenuation. All three scatter methods are limited to the determination of convex body contours.

The effect of boundary error on the postreconstruction correction matrix method (*8*) of attenuation compensation in SPECT is demonstrated for the 22-cm diameter cylindrical phantom filled with a uniform concentration of ^{99m}Tc solution (Fig. 6). Displacement of 1 pixel (6 mm) of a correctly sized attenuation compensation matrix along the diameter of the cylinder resulted in a distorted count profile in the final corrected image. Boundary errors leading to under-or overestimation of the size of the correction matrix cause similar distortions in SPECT quantitations. Using an attenuation coefficient of 0.15, calculations of the multiplicative factor for the central pixel of the 22 cm cylinder will be erroneous by ~9% for 1 pixel and 16% for 2 pixels under- or overestimation of the size of the correction matrix. This corresponds to misestimation of the section diameter by 1.2 and 2.4 cm, respectively (Fig. 7A). Figure 7A illustrates the effects of other under- or overestimates of the size of the correction matrix for the 22-cm cylinder. Furthermore, the magnitude of the fractional quantitative error for the central pixel is essentially independent of the diameter of the section or object. While this may be surprising initially, it becomes intuitive when one appreciates the nature of

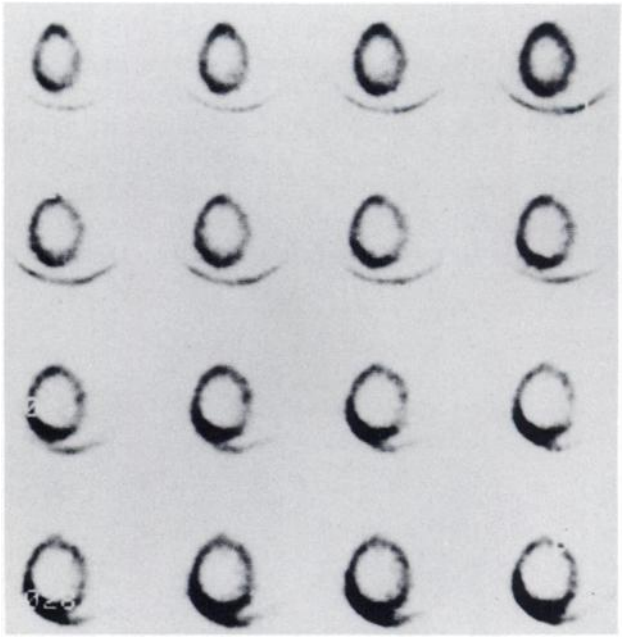

FIGURE 5
Sixteen 12 mm thick transverse section images of the head of a male subject obtained with reconstruction of 90-degree Compton scattered events acquired with 360-degree rotation of the camera. The boundaries of the head are well defined.

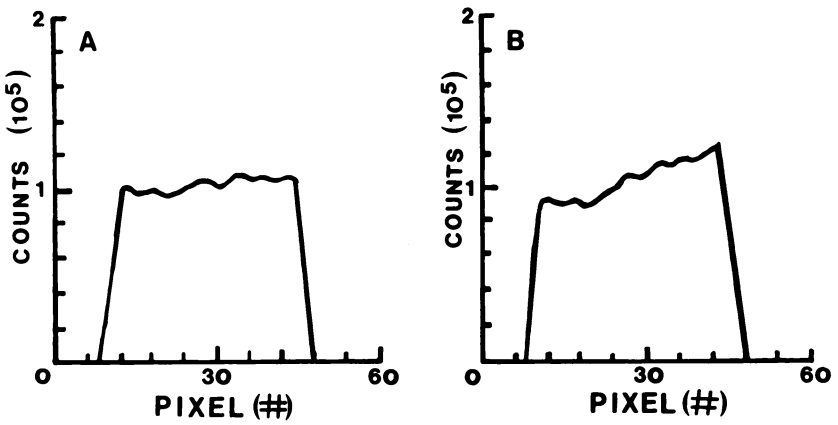

FIGURE 6
Count profiles across a 2.5 cm thick transverse section image of a 22 cm diameter cylinder filled with ^{99m}Tc, in which attenuation compensation had been performed on a postreconstruction matrix that was A: aligned in position and size to the section image; and B: displaced along the horizontal axis by 6 mm. The transverse section images of this phantom were acquired with 360-degree SPECT using a 64 × 64 matrix and 64 projection images. Positional misalignment introduced serious error.

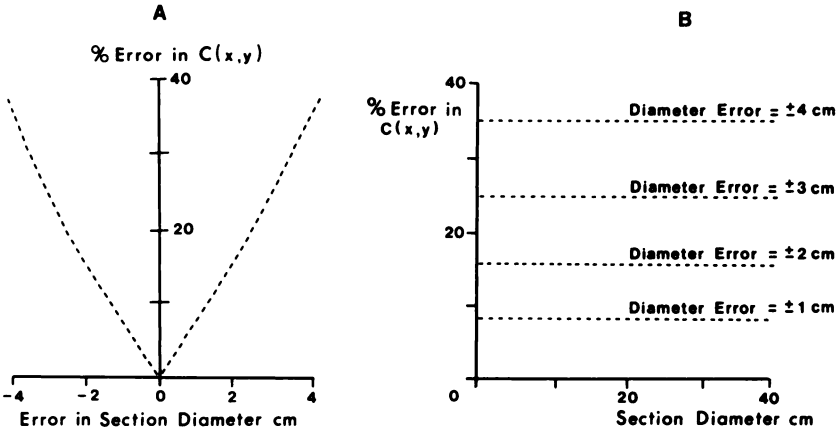

FIGURE 7
Variation in the fractional error of the multiplicative factor, C(x.y), for the central pixel of the post reconstruction correction matrix with misestimation of the size of the correction matrix for: A: A 22 cm diameter section such as the cylinder of water; and, B: Sections (objects) of larger or smaller diameters. Boundary errors had a significant influence on the quantitations (A), and the magnitude of this influence was surprisingly independent of the diameter of the section (B).

the function for calculating the correction matrix (exp (-u*x)). These results confirm that accurate definition of the boundaries of the correction matrix relative to their location and size is essential for accurate SPECT quantitations and important for qualitative SPECT images. The 90-degree Compton scatter method described in this article provided sufficiently good boundary information to permit accurate definition of the location and size of the boundaries of several objects including a lucite phantom and the head and abdomen of a male subject.

ACKNOWLEDGMENTS

This work was supported by Department Of Energy Grant #DE FG03-84ER60233 and American Cancer Society Grant #PDST-94H.

REFERENCES

1. Gullberg GT, Malko JA, Eisner RL. Boundary detection methods for attenuation correction in single photon emission computed tomography. In: Esser P, ed. *Emission computed tomography: current trends.* New York: The Society of Nuclear Medicine, 1983:33–53.
2. Budinger TF, Gullberg GT, Huesman HH. In *Image reconstruction from projections.* New York: Springer-Verlag. 1979:207–219.
3. Larson SA. Gamma camera emission tomography. *Acta Radiologic* 1980; NB (suppl 363):1–75.
4. Jaszczak RJ, Chang LT, Stein NA, et al. Whole body single photon emission computed tomography using large field of view scintillation cameras. *Phys Med Biol* 1979; 24:1123–1143.
5. Webb S, Flower MA, Ott RJ, et al. A comparison of attenuation correction methods for quantitative single photon emission computed tomography. *Phys Med Biol* 1983; 28:1045–1056.
6. Hosoba M, Wani H, Toyoma H, et al. Automated body contour detection in SPECT: effects on quantitative studies. *J Nucl Med* 1986; 27:1184–1191.
7. Hawmann EG. Impact of body contour data on quantitative SPECT imaging. *Proceedings of the Third World Congress of Nuc Med Biol* Vol 1. Raynaud C, ed. Paris: Perganon Press, 1982:1038–1041.
8. Chang LT. A method for attenuation correction in radionuclide computed tomography. *IEEE Trans Nuc Sci* 1978; NS-25:638–642.